Oxidation States of Gold in MgO-Supported Complexes and Clusters: Characterization by X-ray Absorption Spectroscopy and Temperature-Programmed Oxidation and Reduction

Javier Guzman and Bruce C. Gates*

Department of Chemical Engineering and Materials Science, University of California, Davis, California 95616

Received: September 12, 2002; In Final Form: December 11, 2002

X-ray absorption near edge structure (XANES) spectroscopy, temperature-programmed reduction (TPR), and temperature-programmed oxidation (TPO) were used in combination to determine the oxidation states of gold in clusters and complexes supported on MgO. The samples were also characterized by X-ray absorption fine structure (EXAFS) spectroscopy to determine the structure of the supported gold species. The samples were prepared by adsorption of $Au^{III}(CH_3)_2(C_5H_7O_2)$ on MgO followed by treatment in He or H_2 for 2 h at 573 K and 1 atm. The XANES and TPR results identify Au^{3+} in supported gold complexes and show that treatment in H_2 caused reduction at 480 K to metallic gold, which could be reoxidized to Au^{3+} at about 490 K by treatment in O_2, as shown by TPO and XANES. Treatment of the sample containing supported Au(III) complexes with CO led to the formation of partially reduced gold (Au^+, 40 ± 5%) and zerovalent gold (60 ± 5%), as shown by the combination of XANES, TPR, and TPO. The results demonstrate how XANES and TPR/TPO used in combination can effectively determine the oxidation states of metals on supports, even when the metals are present in various oxidation states.

Introduction

Small supported gold clusters have been inferred to be active catalysts for reactions including CO oxidation,[1−3] the water gas shift,[4] and NO reduction,[5] as well as selective catalysts for oxidation of propene to propene oxide[6,7] and hydrogenation of acetylene.[8] The properties of these catalysts, which depend on the support,[9] synthesis method,[10] and pretreatment conditions,[11] have been variously attributed to the smallness of the gold clusters[10,12] and to the simultaneous presence of metallic gold atoms adjacent to cationic gold,[13−15] but the nature of the active sites and the oxidation state(s) of gold remain to be fully elucidated.

The oxidation states of supported gold have been characterized by X-ray absorption near edge structure (XANES)[16,17] and temperature-programmed reduction (TPR)[18,19] and oxidation (TPO).[20] XANES is the only one of these techniques that can be used to follow changes in the oxidation state of gold under catalytic reaction conditions. Such in-situ experiments are valuable because the state of the gold is expected to depend on the reaction conditions. However, the quantitative interpretation of XANES remains challenging, although the fundamental multiple-scattering (MS) theory of X-ray absorption is well established.[21−23] On one hand, the lack of self-consistent-field potentials and the large basis size requirements in existing MS codes make them of limited accuracy; on the other hand, conventional ground-state electronic structure methods usually depend on lattice periodicity or neglect core-hole and self-energy effects.[23,24] Therefore, there is a strong motivation to use additional techniques that quantify the oxidation states of gold in combination with XANES. TPR and TPO quantitatively determine average oxidation states of supported metals,[25−27] and these techniques appear to be ideal complements of XANES for the quantitative determination of the oxidation states of gold.

The goal of the research presented here was to use XANES, TPO, and TPR in combination to characterize a family of supported samples incorporating gold complexes and gold clusters of various sizes to demonstrate how these techniques complement each other in determining the gold oxidation states. We report MgO-supported gold catalysts prepared from $Au^{III}(CH_3)_2$(acac) (acac is $C_5H_7O_2$, acetylacetonate). The results give evidence of a range of oxidation states of gold in the catalysts depending on the treatment conditions; they demonstrate how TPR, TPO, and XANES used in combination determine quantitatively the oxidation states of gold in supported catalysts.

Experimental Section

Materials. H_2 was supplied by Matheson (99.999%) or generated by electrolysis of water in a Balston generator (99.99%) and purified by passage through traps containing reduced Cu/Al_2O_3 and activated zeolite 4A to remove traces of O_2 and moisture, respectively. He (Matheson, 99.999%) was purified by passage through similar traps. The reactant gases, O_2 (Matheson, 99.999%) in a 5% mixture in He, and H_2 (Matheson, 99.999%) in a 5% mixture in Ar, were used as received. CO (Matheson, 99.999%), in a 10% mixture in He, was purified by passage through a trap containing activated γ-Al_2O_3 particles and zeolite 4A to remove any traces of metal carbonyls from the high-pressure gas cylinder and moisture, respectively. The MgO support (EM Science, 97%, BET surface area, 60 $m^2\ g^{-1}$) was calcined in O_2 at 673 K for 2 h, isolated, and stored in a drybox until it was used. *n*-Pentane solvent (Fisher, 99%) was dried and purified by refluxing over sodium benzophenone ketyl and deoxygenated by sparging of N_2. The precursor $Au(CH_3)_2$(acac) [dimethyl(acetylacetonate) gold(III)] (Strem, 98%) and the reference compounds AuCl (Strem, 97%), Au_2O_3 (Strem, 99%), and $HAuCl_4$ (Strem, 99%) were used as supplied.

Sample Preparation. The syntheses and transfers of the MgO-supported gold samples, described elsewhere,[15,28] were

* To whom correspondence should be addressed.

10.1021/jp026976a CCC: $25.00
Published on Web 02/15/2003

TABLE 1: EXAFS Parameters Characterizing MgO-Supported Gold Complexes Formed by Adsorption of $Au(CH_3)_2(acac)$ on MgO and Subsequently Treated in He or H_2 at 573 K and a Pressure of 760 Torr[a]

	treatment gas											
	none				He				H_2			
backscatterer	N	R, Å	$10^3\ \Delta\sigma^2$, Å^2	ΔE_0, eV	N	R, Å	$10^3\ \Delta\sigma^2$, Å^2	ΔE_0, eV	N	R, Å	$10^3\ \Delta\sigma^2$, Å^2	ΔE_0, eV
Au												
1st shell	*b*				9.4	2.86	5.97	0.06	9.4	2.85	6.12	1.31
2nd shell	*b*				3.4	4.05	2.36	4.73	4.0	4.05	1.24	4.21
support												
O_s	2.1	2.16	0.20	3.45	1.1	2.17	5.91	6.41	1.2	2.16	11.21	6.51
O_l	0.9	2.85	1.04	1.02	0.9	2.81	2.19	7.44	1.0	2.87	0.17	12.88
Mg	0.9	2.72	1.09	3.05	0.9	2.75	3.26	0.73	0.7	2.78	7.21	8.53

[a] Notation: N, coordination number; R, distance between absorber and backscatterer atoms; $\Delta\sigma^2$, Debye−Waller factor; ΔE_0, inner potential correction. Expected errors: N, ±10%; R, ±0.02 Å; $\Delta\sigma^2$, ±20%; ΔE_0, ±20%. The subscripts s and l refer to short and long, respectively. [b] Undetectable.

performed in the absence of moisture and air. The samples were prepared by slurrying $Au(CH_3)_2(acac)$ in dried and deoxygenated *n*-pentane with partially dehydroxylated MgO powder that had been pretreated at 673 K in a vacuum. The slurry was stirred for 1 day and the solvent removed by evacuation. The resultant MgO-supported gold sample, containing 1.0 wt % Au, was treated in flowing He or H_2 at 573 K.

TPR. TPR experiments were performed with an RXM-100 multifunctional catalyst testing and characterization system (Advanced Scientific Designs, Inc.) with a vacuum capability of 10^{-9} Torr; it was equipped with a thermal conductivity detector (TCD). In a N_2-filled drybox, the sample for TPR (typically 0.3−0.5 g) was weighed, loaded into a quartz tube, sealed, and transferred to the characterization system without exposure to air or moisture. Prior to each experiment, the sample was pretreated at room temperature in flowing Ar [10 mL (NTP) min^{-1}] for 20 min. The sample powder was treated by heating from 298 to 1073 K at a rate of 10 K min^{-1} in a flow of 5 vol % H_2 in Ar or in a flow of 5 vol % CO in He. The total gas flow rate was 10 mL (NTP) min^{-1}. The experimental parameters were chosen so that the "*K* number" (defined[29] as the ratio of reducible substance (mol) divided by the H_2 flow rate (mol s^{-1})) had a value in the range 55−140 s. The TCD signal was calibrated to determine H_2 consumptions by using the complete reduction of CuO powder as a standard (Aldrich, 99.995%) and by measuring the area under the TCD signal for known H_2 and CO concentrations. The H_2 and CO uptakes were determined with an accuracy of about ±10%.[30]

TPO. TPO experiments were performed similarly in the same characterization system. The sample (typically 0.3−0.5 g) was treated by heating from 298 to 1073 K at a rate of 10 K min^{-1} in a flow of 5 vol % O_2 in He. The total gas flow rate was 10 mL (NTP) min^{-1}. A TPO experiment was performed after each TPR experiment, once the sample had been cooled to room temperature in flowing Ar (10 mL (NTP) min^{-1}). A series of TPR experiments was performed after TPO tests, once the sample had been cooled to room temperature in flowing He (10 mL (NTP) min^{-1}). The O_2 uptakes were determined with an accuracy of about ±10%.[31]

X-ray Absorption Spectroscopy (XAS). XANES and extended X-ray absorption fine structure (EXAFS) experiments were performed on Beamline 4-1 of the Stanford Synchrotron Radiation Laboratory (SSRL) at the Stanford Linear Accelerator Center, Stanford, CA. The storage ring electron energy was 3 GeV, and the ring current varied within the range 50−100 mA. In a N_2-filled drybox at the synchrotron, powder samples were loaded into an in-situ XAS cell,[32] which was then aligned in the X-ray beam. XAS spectra were recorded for each sample in transmission mode at the Au L_{III} edge (11 919 eV) at atmospheric pressure and at room temperature. In the in-situ XANES experiments, the data were collected during treatment of the supported sample in flowing H_2 or CO, as a spectrum in the energy range 11 880−12 000 eV was recorded every 2 min while the temperature was ramped up at a rate of 2 K/min. Details of the sample handling are as described elsewhere.[33,34] The higher harmonics in the X-ray beam were minimized by detuning the Si(220) monochromator by 20−25% at the Au L_{III} edge.

EXAFS Data Analysis. Analysis of the EXAFS data was carried out with a difference file technique with experimentally and theoretically determined reference files; details of the preparation of the reference files[35,36] and data analysis procedures are presented elsewhere.[33,37] The data were analyzed with the software XDAP.[38] The X-ray absorption edge energy was calibrated with the measured signal of a gold foil (at the Au L_{III} edge (11 919 eV)) that was scanned simultaneously with the sample. The edge is represented as the inflection point at the first absorption peak, at nearly 11 919 eV. The data were normalized by dividing the absorption intensity by the height of the absorption edge.

Results

EXAFS Evidence of Gold Complexes and Clusters on MgO. EXAFS spectroscopy was used to characterize the structures of the gold complexes formed by adsorption of $Au(CH_3)_2(acac)$ on MgO and the gold clusters formed by treatment of these complexes in flowing He or H_2 at 573 K for 2 h. The EXAFS parameters (Table 1) characterizing the sample formed by adsorption of $Au(CH_3)_2(acac)$ on MgO powder show that site-isolated mononuclear gold complexes were the predominant surface species, as demonstrated by the lack of Au−Au first- and second-shell coordination numbers *N*. No Au−Au contributions were found at typical Au−Au bond distances (2.86 Å), consistent with the inference that the supported species were site-isolated and mononuclear.[39]

Two other samples were prepared by adsorption of $Au(CH_3)_2(acac)$ on MgO, followed by treatment in flowing He or H_2 at 573 K for 2 h. The data representing these samples (Table 1) demonstrate the presence of gold in the form of clusters with an average diameter of about 30 Å; these contained about 200 Au atoms each, on average, as determined from models[40,41] that relate the average cluster size to the EXAFS first- and second-shell Au−Au coordination numbers, which were 9.4 ± 0.9 and 3.5 ± 0.4, respectively, for the sample treated in flowing He and 9.4 ± 0.9 and 4.0 ± 0.4, respectively, for the sample treated in flowing H_2.[28]

XANES. XANES data provide information about the oxidation states of the gold species. XANES peak locations and

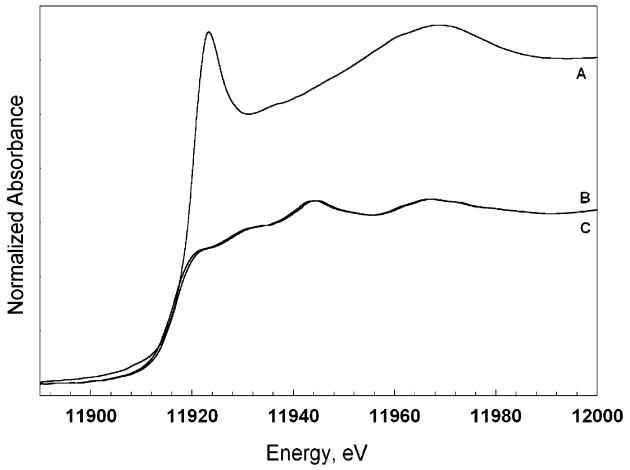

Figure 1. XANES characterizing MgO-supported gold samples: (A) mononuclear Au(III) complexes; (B) gold clusters formed by treatment in He at 573 K; (C) gold clusters formed by treatment in H_2 at 573 K. The samples were scanned at liquid nitrogen temperature under vacuum (10^{-5} Torr).

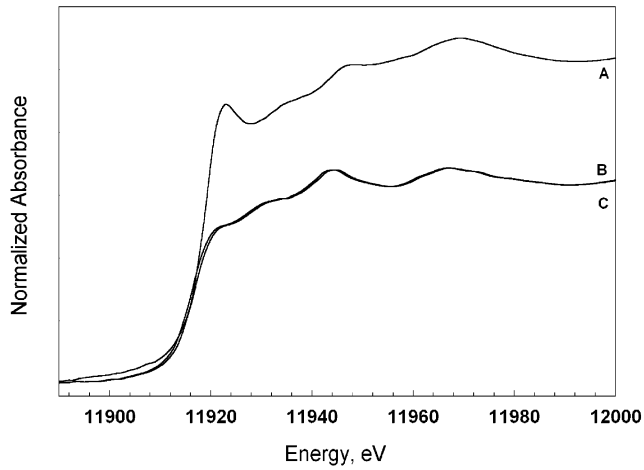

Figure 2. XANES characterizing MgO-supported gold samples during exposure to CO (P_{CO} = 11 Torr) at 473 K: (A) mononuclear Au(III) complexes; (B) gold clusters formed by treatment in He at 573 K; (C) gold clusters formed by treatment in H_2 at 573 K.

intensities characterizing reference materials containing gold in various oxidation states, summarized elsewhere,[15−17] provide a basis for interpretation of the data.

Data representing the supported mononuclear gold complex include an intense peak at 4 eV (the white line), a shoulder at 15 eV, and a broad shoulder at 50 eV higher than the edge (Figure 1). These peaks and their intensities match the features characterizing Au(III) in $Au(CH_3)_2$(acac), $HAuCl_4$, and Au_2O_3.[15−17] Thus, we conclude that the gold in the supported sample was Au(III). In contrast, the XANES data representing samples containing gold clusters with an average diameter of about 30 Å show the complete absence of the 4-eV peak and intense peaks at 15, 25, and 50 eV above the edge (Figure 1). These spectra virtually match that of metallic gold foil.[15−17] Thus, the comparison of the XANES of zerovalent gold and that in the samples containing gold clusters shows that the gold in these supported samples was Au(0).

The samples were exposed to CO to determine its influence on the oxidation state of the gold. Exposure of the sample containing mononuclear Au(III) complexes to CO (P_{CO} = 11 Torr) at 473 K resulted in a decrease in intensity of the 4-eV peak and the appearance of an intense peak at 25 eV as well as peaks at 15 and 50 eV above the edge (Figure 2). A comparison of the spectrum with those of AuCl[17] and $(PPh_3)AuCl$[16] (each containing Au(I)) and with that of metallic gold[15] indicates the presence of both Au(I) and Au(0). The data demonstrate a reduction of the white line intensity as a result of the CO treatment − but without its complete disappearance, as would be expected if all the gold had been converted into the zerovalent form. The white line intensity suggests the presence of gold in an intermediate oxidation state, expected, on the basis of the chemistry of gold, to be Au(I).[13,15] The peaks at 15 and 25 eV are characteristic of metallic gold. Consistent with these results, we recently reported the simultaneous presence of Au(I) and Au(0) in functioning MgO-supported CO oxidation catalysts, as indicated by XANES spectroscopy.[15]

When samples containing gold clusters were exposed to CO (P_{CO} = 11 Torr) at 473 K (Figure 2), the XANES remained indistinguishable from that of the sample before CO treatment. Thus, the data indicate the presence of zerovalent gold before and after CO treatment.

TPR in H_2. TPR profiles characterizing the reference compounds AuCl, Au_2O_3, $HAuCl_4$, and $Au(CH_3)_2$(acac)—each physically mixed with inert γ-Al_2O_3—were determined, as well as the H_2 uptake (calculated by integrating the area under the TCD signal and on the basis of the calibration) for each reduction process observed in the samples (Table 2). The measured H_2 uptakes for reduction of Au(III), contained in $Au(CH_3)_2$(acac), Au_2O_3, or $HAuCl_4$, agree with the number of electrons necessary for the stoichiometric reduction Au(III) → Au(0):

$$Au^{3+} + 3e^- \rightarrow Au^0 \quad (1)$$

Similarly, the H_2 uptake of the reference compound AuCl agrees with the value expected for complete reduction of Au(I) to Au(0). These and related data summarized in Table 2 provide a basis for interpretation of the TPR profiles of our supported gold samples.

TABLE 2: H_2 Uptake during Reduction of Gold from Various Oxidation States[a]

sample	reduction process	H_2 uptake (mol of H_2 (mol of Au)$^{-1}$) stoichiometric	experimental
$Au(CH_3)_2$(acac)	$Au^{3+} \rightarrow Au^0$	1.50	1.54
Au_2O_3	$Au^{3+} \rightarrow Au^0$	1.50	1.48
$HAuCl_4$	$Au^{3+} \rightarrow Au^0$	1.50	1.51
b	$Au^{2+} \rightarrow Au^0$	1.00	
AuCl	$Au^{+} \rightarrow Au^0$	0.50	0.52
$(PPh_3)AuCl$	$Au^{+} \rightarrow Au^0$	0.50	0.54

[a] Calculated on the basis of the assumption that each H_2 molecule contributes $2e^-$ to the reduction process and assuming that all of the cationic gold is present as Au^{3+}, Au^{2+}, or Au^+. [b] Calculated value only.

TPR profiles are shown in Figure 3 for bare MgO that had been calcined at 673 K, various supported gold samples, and the precursor $Au(CH_3)_2$(acac). As expected, the TPR profile of bare MgO does not show any reduction peak in the temperature range 300−673 K. The TPR profile characterizing $Au(CH_3)_2$(acac) includes a reduction peak at 421 K, with a H_2 uptake of 1.53 ± 0.15 mol of H_2 (mol of Au)$^{-1}$, corresponding to complete conversion of Au(III) to Au(0). The TPR results characterizing the sample containing supported mononuclear gold complexes show a peak at 481 K (Table 3). The observed H_2 uptake of 1.51 ± 0.15 mol of H_2 (mol of Au)$^{-1}$ corresponds to complete reduction of Au(III) to Au(0).

The data thus indicate that upon adsorption of $Au(CH_3)_2$(acac) on MgO, the gold remained as Au(III) in the resultant

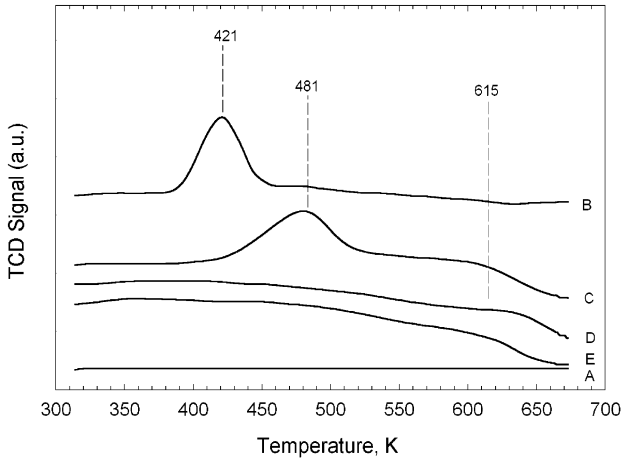

Figure 3. TPR profiles characterizing the following samples: (A) MgO; (B) the precursor $Au(CH_3)_2(acac)$; (C) the MgO-supported sample prepared by adsorption of $Au(CH_3)_2(acac)$; (D) the preceding sample after treatment in flowing He at 573 K; (E) the sample represented in C after treatment in flowing H_2 at 573 K.

TABLE 3: Results of TPR Experiments Characterizing MgO-Supported Gold Samples and Reference Materials[a]

sample	pretreatment gas	pretreatment temp, K	H_2 consumption (mol of H_2 (mol of Au)$^{-1}$)	reduction temp, K
MgO	none	none	0	none
$Au(CH_3)_2(acac)$	none	none	1.53	421
$[Au(CH_3)_2]/MgO$	none	none	1.51	481
Au/MgO[b]	He	573	0	none
Au/MgO[b]	H_2	573	0	none

[a] Data determined for samples containing 1 ± 0.1 wt % Au and assuming that all of the cationic gold was present either as Au^{3+} or Au^0. [b] Sample that initially contained larger (aggregated) clusters, with an average diameter of about 30 Å.

supported mononuclear gold complex, consistent with the XANES results. When the sample was treated in flowing H_2, complete reduction to Au(0) occurred at 481 K. The temperature of the reduction of Au(III) to Au(0) in our sample agrees well with that characterizing the reduction of Au(III) to Au(0) in Fe_2O_3-supported gold samples (489 K).[18]

The TPR profiles characterizing the samples containing gold clusters do not show any reduction peaks in the temperature range 300−673 K (Figure 3), confirming that the gold in the clusters was present as Au(0).[42]

TPO. TPO profiles characterizing the MgO-supported samples incorporating mononuclear Au(III) complexes and those incorporating zerovalent gold clusters are shown in Figure 4. The data characterizing the latter samples include a peak at 490 K with desorption of oxygen (or release of other gaseous products) observed at 625 K. These TPO results are consistent with the presence of zerovalent gold in the samples containing gold clusters (which had been reduced by pretreatment in He or H_2 at 573 K). The oxygen uptakes (0.73 ± 0.07 and 0.77 ± 0.07 mol of O_2 (mol of Au)$^{-1}$, for the samples treated in He and H_2, respectively) agree with the stoichiometric amount of oxygen (0.75 mol of O_2 (mol of Au)$^{-1}$) necessary for the complete oxidation of zerovalent gold, represented as follows:

$$Au^0 - 3e^- \rightarrow Au^{3+} \qquad (2)$$

They indicate that all the gold in these samples prior to the oxidation was zerovalent. The oxidation occurs at a temperature, 490 K, nearly the same as that observed for the reduction of

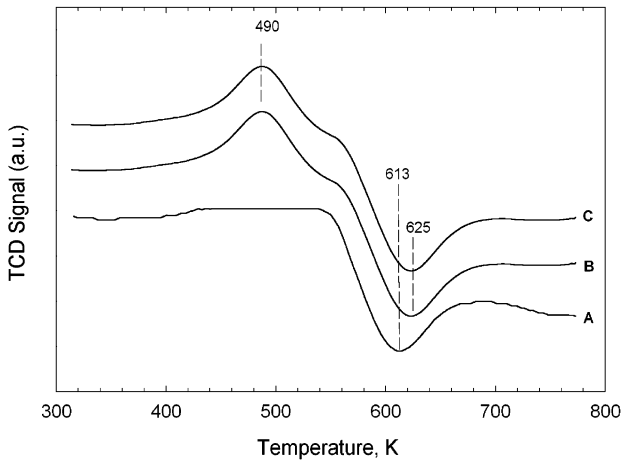

Figure 4. TPO profiles characterizing the following samples: (A) the MgO-supported sample prepared by adsorption of $Au(CH_3)_2(acac)$; (B) the preceding sample after treatment in flowing He at 573 K; (C) the sample represented in B after treatment in flowing H_2 at 573 K.

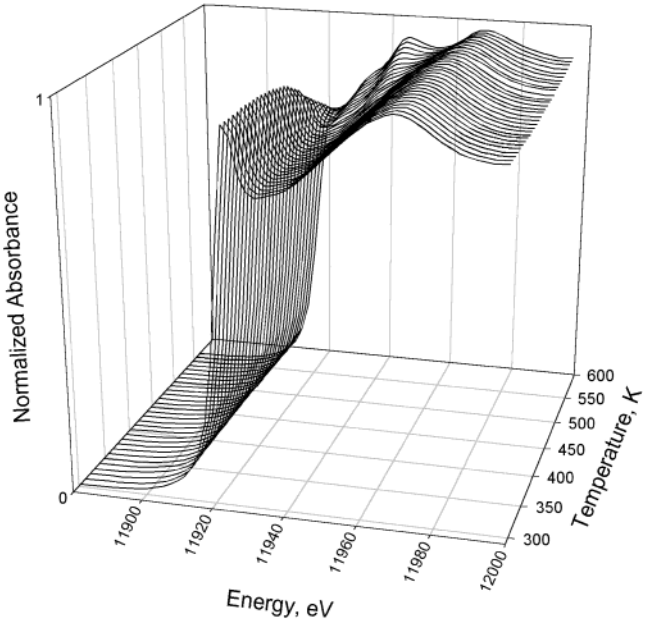

Figure 5. XANES data characterizing the H_2-TPR of the MgO-supported sample (prepared by adsorption of $Au(CH_3)_2(acac)$) in a flow of 5 vol % H_2 in He while the temperature was ramped up at a rate of 2 K/min.

Au(III) to Au(0) (481 K) in the supported sample formed by adsorption of $Au(CH_3)_2(acac)$.

The TPO data characterizing the sample initially incorporating mononuclear gold complexes do not include any peak indicating oxidation. The data simply show an oxygen desorption peak at 613−625 K, attributed to desorption of oxygen from the MgO support (which had been calcined in O_2 at 673 K) or possibly to decomposition of carbonaceous species formed on the MgO during the synthesis.[43] The lack of any oxidation peak in the spectrum confirms the presence of gold in its highest stable oxidation state, Au(III).[44]

XANES Recorded during TPR of Supported Au(III). The XANES data collected during the TPR in H_2 of the sample initially containing mononuclear Au(III) (Figure 5) show a gradual decrease in intensity of the 4-eV peak, indicating reduction of Au(III), until it disappeared at approximately 530 K, indicating the conversion of all the gold to the zerovalent state. This conclusion is supported by the appearance of XANES

TABLE 4: Comparison of XANES and TPR Results Characterizing Reduction of Au(III) to Au(0)

method of determination of reductn from Au(III) to Au(0)	obsd temp, K		
	initial	maximum	final
XANES	450	490	530
TPR	440	481	518

features typical of metallic gold at 15 and 25 eV above the edge at temperatures higher than 450 K. A summary of the temperature ranges of the reduction process observed in the spectra is shown in Table 4.

To investigate the structure of the gold species formed during this in-situ XANES-TPR experiment, EXAFS spectra were recorded at the end of the experiment. The data (Table 5) indicate the presence of clusters of gold with an average diameter of about 30 Å, as determined from the Au−Au first- and second-shell coordination numbers of 9.1 ± 0.9 and 3.0 ± 0.3, respectively. The results confirm those stated above for the samples formed by adsorption of $Au(CH_3)_2(acac)$ followed by treatment in H_2 at 573 K.

In contrast, the EXAFS results collected at the end of a XANES-TPO experiment characterizing the sample initially containing zerovalent gold clusters indicate partial fragmentation of the clusters, as shown by the decrease in the Au−Au first- and second-shell coordination numbers (5.1 ± 0.5 and 2.1 ± 0.2; Table 5) relative to those characterizing the sample before the experiment (9.4 ± 0.9 and 4.0 ± 0.4; Table 1). Furthermore, the EXAFS data, consistent with the TPO results, indicate oxidation of the gold, as shown by the increased Au−O contributions in the EXAFS spectra (Tables 1 and 5).

TPR in CO. TPR experiments with CO were performed to quantify the influence of CO on the redox chemistry of gold. The CO-TPR profiles characterizing the MgO-supported gold samples are shown in Figure 6. As shown by the XANES and H_2-TPR data, the CO-TPR results characterizing the samples that initially contained gold clusters demonstrate the presence of zerovalent gold, as indicated by the absence of any peak associated with reduction of gold. In contrast, the data characterizing the sample that initially contained mononuclear Au(III) show an uptake of CO (1.30 ± 0.13 mol of CO (mol of Au)$^{-1}$) at about 483 K, attributed to the reduction of Au(III). The stoichiometric CO consumption for reduction of Au(III) to Au(0) is 1.5 mol of CO (mol of Au)$^{-1}$. The observed CO uptake by our sample corresponds to less than complete reduction of the Au(III) to Au(0); the data imply reduction of at least some of the Au(III) to an intermediate oxidation state—indicated by the XANES to be Au(I). The CO consumed cannot be attributed exclusively to reduction of Au(III) to Au(I), because the uptake was more than enough for this conversion.

A fraction of the Au(III) must have been reduced to zerovalent gold. On the basis of the XANES results indicating the presence

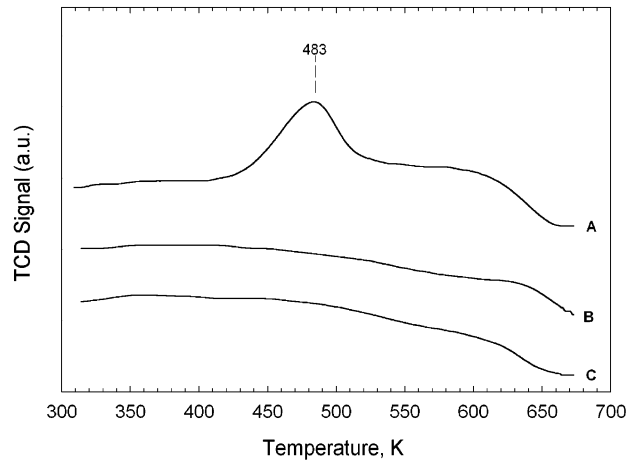

Figure 6. CO-TPR profiles characterizing the following samples: (A) the MgO-supported sample prepared by adsorption of $Au(CH_3)_2(acac)$; (B) the preceding sample after treatment in flowing He at 573 K; (C) the sample represented in A after treatment in flowing H_2 at 573 K.

of Au(I) and Au(0), combined with the CO consumption, we infer the stoichiometry of the reduction of gold to be as follows:

$$Au^{3+} + (3 - x)e^- \rightarrow xAu^+ + (1 - x)Au^0;\ 0 < x < 1 \quad (3)$$

The uptake data show that treatment of the sample containing mononuclear Au(III) complexes in CO led to the formation of a mixture of 40 ± 5% Au^+ and 60 ± 5% zerovalent gold. The distribution of gold oxidation states depends on the treatment conditions.[45]

TPO after CO-TPR. The TPO profiles characterizing the MgO-supported gold samples after CO-TPR are shown in Figure 7. The TPO data characterizing the samples that contained zerovalent gold clusters that had been investigated by CO-TPR experiments show a peak at 495 K indicating oxidation and another, negative, peak indicating oxygen desorption or perhaps the release of gaseous products at 613 K. The data indicate the complete oxidation of Au(0) to Au(III), as demonstrated by the measured uptake of 0.78 ± 0.07 mol of O_2 (mol of Au)$^{-1}$, which agrees with the stoichiometric amount of oxygen (0.75 mol of O_2 (mol of Au)$^{-1}$) for the complete conversion of Au(0) to Au(III). In contrast, the TPO data characterizing the sample that initially contained mononuclear gold after CO-TPR to form a mixture of Au(I) and Au(0) show a shoulder at about 495−500 K. The observed uptake was 0.60 ± 0.06 mol of O_2 (mol of Au)$^{-1}$, indicating only partial oxidation of the gold (the stoichiometric amount of oxygen necessary for the complete oxidation of metallic gold to Au(III) is 0.75 mol of O_2 (mol of Au)$^{-1}$). This peak was not observed during TPO of the sample that initially contained all of the gold as Au(III). Thus, we infer the presence of some of the gold in an intermediate oxidation state, consistent with the XANES and CO-TPR results. There-

TABLE 5: EXAFS Parameters Characterizing MgO-Supported Gold Formed after in Situ XANES during H_2-TPR and O_2-TPO[a]

	H_2-TPR				O_2-TPO			
backscatterer	N	R, Å	$10^3\Delta\sigma^2$, Å^2	ΔE_0, eV	N	R, Å	$10^3\Delta\sigma^2$, Å^2	ΔE_0, eV
Au								
1st shell	9.1	2.85	5.23	1.74	5.1	2.83	7.01	3.21
2nd shell	3.0	4.04	3.53	2.34	2.1	4.09	1.41	0.12
support								
O_s	1.0	2.15	4.84	5.12	2.4	2.17	6.63	0.33
O_l	0.0	2.86	1.78	7.21	1.5	2.80	8.74	5.35
Mg	0.7	2.74	4.23	4.14	0.8	2.78	3.98	2.00

[a] Notation as in Table 1.

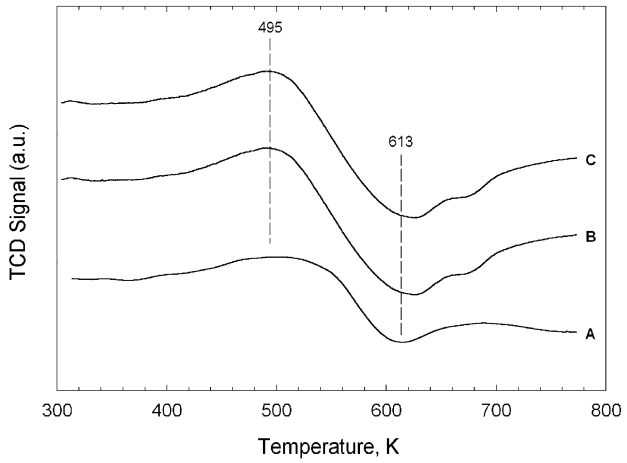

Figure 7. TPO profiles characterizing the following samples after CO-TPR: (A) the MgO-supported sample prepared by adsorption of Au-$(CH_3)_2$(acac); (B) the preceding sample after treatment in flowing He at 573 K; (C) the sample represented in A after treatment in flowing H_2 at 573 K.

fore, these results show that treatment of the sample containing mononuclear Au(III) complexes in CO led to the formation of a mixture of 42 ± 5% Au^+ and 58 ± 5% zerovalent gold, consistent with the CO-TPR results.

Discussion

Oxidation States of Gold. The XANES, TPR, and TPO results characterizing the oxidation state of gold in the supported samples show internal agreement within the experimental error, identifying Au(III) and Au(0) independently. The fact that XANES and TPR determine the temperature ranges of reduction of the gold with an uncertainty of only ±10 K (Table 4) shows that these two techniques can be used for accurate monitoring of changes in the oxidation states of supported metals.[46] Quantitative interpretation of TPR experiments characterizing Au/Fe_2O_3,[18] VO_x/Al_2O_3,[47] $Co_2(CO)_8/\gamma\text{-}Al_2O_3$,[48] and V_2O_5/TiO_2,[49] for example, demonstrates the effectiveness of TPR for the determination of H/M ratios in supported metals.

Our results demonstrate the usefulness of XANES, TPR, and TPO used in concert to quantify the gold in various oxidation states on a support. TPR and TPO used together (or alone), are not sufficient, because the CO, H_2, and O_2 uptakes cannot be attributed exclusively to single redox processes, and the data provide only average oxidation states of the gold. But XANES determines qualitatively which oxidation states of gold are present, and the combination of XANES with TPR and/or TPO allows a full determination of the oxidation states of the gold.

Aggregation and Fragmentation of Gold Clusters during Reduction and Oxidation. The data show that the reduction−oxidation of gold from Au(III) to Au(0) is a reversible process occurring at 480−490 K. The EXAFS data provide evidence of aggregation and fragmentation during changes in the oxidation state of gold. Reduction of Au(III) to Au(0) in the sample that initially contained mononuclear Au(III) complexes led to aggregation of the gold, as demonstrated by an increase in the Au−Au first- and second-shell coordination numbers in the EXAFS data recorded at the end of in-situ XANES collected during H_2-TPR (Table 5). Similarly, the aggregation of metal clusters on MgO during H_2 treatment at various temperatures has been demonstrated, for example, for clusters approximated as Ir_4[50−52] and Ir_6.[53,54]

In contrast, oxidation of Au(0) to Au(III) in the sample that initially contained gold clusters (formed by pretreatment in H_2 at 573 K) led to an oxidative fragmentation of the clusters, as demonstrated by the EXAFS data recorded at the end of the collection of the in-situ XANES data during O_2-TPO, which show a decrease in the Au−Au coordination number and an increase in the Au−O contributions. This fragmentation was not complete, and the resultant oxidized species were not the same as those present in the initially prepared samples as Au-(III) complexes. Instead, these oxidized species are not well-defined structurally, consisting of oxidized and aggregated species that might be regarded as gold oxide clusters. Consistent with this suggestion, oxidative fragmentation of Rh_6 and Ir_4 clusters supported on MgO[55] led to the formation of metal oxide like species under conditions similar to those reported here. Comparable results have been observed for the oxidative fragmentation of $[Rh_6(CO)_{15}]^{2-}$ in NaX zeolite,[56] Pt clusters in KLTL zeolite,[57] and Ir clusters on MgO, for example.[57]

Conclusions

Mononuclear Au(III) complexes and zerovalent gold clusters were prepared from $Au^{III}(CH_3)_2$(acac) on MgO powder by adsorption of the precursor and subsequent treatment in flowing He or H_2, respectively. The samples were characterized by X-ray absorption spectroscopy, TPR, and TPO. XANES and TPR data independently indicate the existence of Au(III) in supported gold complexes prepared by adsorption of $Au^{III}(CH_3)_2(C_5H_7O_2)$. Treatment of these in H_2 at approximately 480 K caused reduction of the gold to zerovalent clusters. XANES and TPO data separately demonstrate the presence of zerovalent gold in the samples containing supported clusters that had been formed by treatment of the initial supported Au(III) complexes in He or H_2 at 573 K. Treatment of the sample containing mononuclear Au(III) complexes in CO led to partial reduction and formation of a mixture of Au(I) and Au(0), which were identified by XANES and determined quantitatively by TPR and TPO. The results demonstrate how the combined application of XANES and TPR/TPO determines quantitatively the oxidation states of metals on supports.

Acknowledgment. We thank Felix Lai for helpful discussions. J. Guzman thanks the Fulbright Commission, Conacyt, and the UC-Mexus Program for support. This research was supported by the U.S. Department of Energy, Office of Energy Research, Office of Basic Energy Sciences, Division of Chemical Sciences, Contract FG02-87ER13790. We acknowledge the Stanford Synchrotron Radiation Laboratory (SSRL), operated by Stanford University for the U.S. Department of Energy, Office of Basic Energy Sciences, for access to beam time. We thank the staff of the SSRL for their assistance. The X-ray absorption spectroscopy data were analyzed with the software XDAP.[38]

References and Notes

(1) Haruta, M.; Tsubota, S.; Kobayashi, T.; Kageyama, H.; Genet, M. J.; Delmon, B. *J. Catal.* **1993**, *144*, 175.

(2) Lin, S. D.; Bollinger, M. A.; Vannice, M. A. *Catal. Lett.* **1993**, *17*, 245.

(3) Liu, H.; Kozlov, A. I.; Kozlova, A. P.; Shido, T.; Iwasawa, Y. *Phys. Chem. Chem. Phys.* **1999**, *1*, 2851.

(4) Andreeva, D.; Idakiev, V.; Tabakova, T.; Andreev, A.; Giovanoli, R. *Appl. Catal. A* **1996**, *134*, 275.

(5) Cant, N. W.; Ossipoff, N. J. *Catal. Today* **1997**, *36*, 125.

(6) Stangland, E. E.; Stavens, K. B.; Andres, R. P.; Delgass, W. N. *J. Catal.* **2000**, *191*, 332.

(7) Mul, G.; Zwijnenburg, A.; van der Linden, B.; Makkee, M.; Moulijn, J. A. *J. Catal.* **2001**, *201*, 128.

(8) Jia, J.; Haraki, K.; Kondo, J. N.; Domen, K.; Tamaru, K. *J. Phys. Chem. B* **2000**, *104*, 11153.

(9) Schubert, M. M.; Hackenberg, S.; van Veen, A. C.; Muhler, M.; Plzak, V.; Behm, R. J. *J. Catal.* **2001**, *197*, 113.

(10) Haruta, M. *Catal. Today* **1997**, *36*, 153.

(11) Maciejewski, M.; Fabrizioli, P.; Grunwaldt, J.-D.; Becker, O. S.; Baiker, A. *Phys. Chem. Chem. Phys.* **2001**, *3*, 3846.

(12) Kozlov, A. I.; Kozlova, A. P.; Liu, H.; Iwasawa, Y. *Appl. Catal. A* **1999**, *182*, 9.

(13) Oh, H.-S.; Costello, C. K.; Cheung, C.; Kung, H. H.; Kung, M. C. *Stud. Surf. Sci. Catal.* **2001**, *139*, 375.

(14) Haruta, M.; Daté, M. *Appl. Catal. A* **2001**, *222*, 427.

(15) Guzman, J.; Gates, B. C. *J. Phys. Chem. B*, **2002**, 106, 7659.

(16) Benfiled, R. E.; Grandjean, D.; Kröll, M.; Pugin, R.; Sawitowski, T.; Schmid, G. *J. Phys. Chem. B* **2001**, *105*, 1961.

(17) Salama, T. M.; Shido, T.; Ohnishi, R.; Ichikawa, M. *J. Phys. Chem.* **1996**, *100*, 3688.

(18) Neri, G.; Visco, A. M.; Galvagno, S.; Donato, A.; Panzalorto, M. *Thermochim. Acta* **1999**, *329*, 39.

(19) Chang, C.-K.; Chen, Y.-J.; Yeh, C.-T. *Appl. Catal. A* **1998**, *174*, 13.

(20) Margitfalvi, J. L.; Fási, A.; Hegedüs, M.; Lónyi, F.; Göbölös, S.; Bogdanchikova, N. *Catal. Today* **2002**, *72*, 157.

(21) Bianconi, A. In *X-ray Absorption, Principles, Applications, Techniques of EXAFS, SEXAFS and XANES*; Koningsberger, D. C., Prins, R., Eds.; Wiley: New York, 1988; Chapter 11.

(22) Lloyd, P.; Smith, P. V. *Adv. Phys.* **1972**, *21*, 69.

(23) Ankudinov, A. L.; Ravel, B.; Rehr, J. J.; Conradson, S. D. *Phys. Rev. B* **1998**, *58*, 7565.

(24) Rehr, J. J.; Albers, R. C. *Rev. Mod. Phys.* **2000**, *72*, 621.

(25) Hurst, N. W.; Gentry, S. J.; Jones, A.; McNicol, B. D. *Catal. Rev.—Sci. Eng.* **1982**, *24*, 33.

(26) Jones, A.; McNicol, B. D. *Temperature-programmed reduction for solid materials characterization*; Marcel Dekker: New York, 1986; p 199.

(27) Knözinger, H. Temperature-programmed reduction in *Handbook of Heterogeneous Catalysis*; Ertl, G., Knözinger, H., Weitkamp, J., Eds.; Wiley-VCH: Weinheim, 1997; Part 2, p 676.

(28) Guzman, J.; Gates, B. C. *Nano Lett.* **2001**, *12*, 689.

(29) Monti, D. A. M.; Baiker, A. *J. Catal.*, **1983**, *83*, 323.

(30) The accuracy and reproducibility of the determination of the area under the TCD signal (thus, the H_2, CO, and O_2 uptakes) were evaluated from multiple measurements of the TCD signals representing standards.

(31) The O_2 consumptions were calculated by integrating the area under the TCD signal and on the basis of the calibrations determining TCD responses at various O_2 concentration. The area under the TCD signal and the baseline were calculated by using the software TPCv.4.11, Advanced Scientific Design, Inc., which extrapolates the baseline (with a linear fitting) from 10 to 30 K before any change of about 5% (peak) is detected in the TCD signal.

(32) Odzak, J. F.; Argo, A. M.; Lai, F. S.; Gates, B. C.; Pandya, K.; Feraria, L. *Rev. Sci. Instrum.* **2001**, *72*, 3943.

(33) Kirlin, P. S.; van Zon, F. B. M.; Koningsberger, D. C.; Gates, B. C. *J. Phys. Chem.* **1990,** *94*, 8439.

(34) Kawi, S.; Chang, J.-R.; Gates, B. C. *J. Am. Chem. Soc.* **1993**, *115*, 4830.

(35) van Zon, J. B. A. D.; Koningsberger, D. C.; van't Blik, H. F. J.; Sayers, D. E. *J. Chem. Phys.* **1985**, *82*, 5742.

(36) Duivenvoorden, F. B. M.; Koningsberger, D. C.; Uh, Y. S.; Gates, B. C. *J. Am. Chem. Soc.* **1986**, *108*, 6254.

(37) Weber, W. A.; Gates, B. C. *J. Phys. Chem. B* **1997**, *101*, 10423.

(38) Vaarkamp, M.; Linders, J. C.; Koningsberger, D. C. *Physica B* **1995**, *209*, 159.

(39) Guzman, J.; Gates, B. C. *Angew. Chem., Int. Ed. Engl.* **2003**, *42*, 690.

(40) Kip, B. J.; Duivenvoorden, F. B. M.; Koningsberger, D. C.; Prins, R. *J. Catal.* **1987**, *105*, 26.

(41) Jentys, A.; *Phys. Chem. Chem. Phys.* **1999**, *1*, 4059.

(42) However, we do not rule out the possibility that a small fraction of the gold could be present as cationic gold, either as Au(III) or Au(I).

(43) This oxygen desorption or release of gaseous products such as CO and CO_2 was observed with all of the MgO-supported samples; thus, it is not associated with changes in the oxidation state of gold. CO and CO_2 have thermal conductivities close to that of O_2 with respect to the carrier gas (Kurhinen, M.; Pakkanen, T. A. *Langmuir* **2000**, *16*, 2658.), and so a possible negative TCD signal can be expected during formation of CO and CO_2 upon thermal decomposition of carbonaceous species.

(44) An O_2 uptake would be expected for oxidation of Au(I) to Au(III). Because none was observed, we conclude that the predominant species were Au(III). However, we cannot rule out the possible presence of a small amount of Au(I) formed upon adsorption of $Au(CH_3)_2$(acac) that would have been undetected by TPO.

(45) Guzman, J.; Gates, B. C., unpublished.

(46) Neylon, M. K.; Marshall, C. L.; Kropf, A. J. *J. Am. Chem. Soc.* **2002**, *124*, 5457.

(47) Concepción, P.; Knözinger, H.; López Nieto, J. M.; Martínez-Arias, A. *J. Phys. Chem. B* **2002**, *106*, 2574.

(48) Kurhinen, M.; Pakkanen, T. A. *Langmuir* **2000**, *16*, 2658.

(49) Besselmann, S.; Freitag, C.; Hinrichsen, O., Muhler, M. *Phys. Chem. Chem. Phys.* **2001**, *3*, 4633.

(50) Triantafillou, N. D.; Gates, B. C. *J. Phys. Chem.* **1994**, *98*, 8431.

(51) Xiao, F.-S.; Xu, Z.; Alexeev, O.; Gates, B. C. *J. Phys. Chem.* **1995**, *99*, 1548.

(52) Alexeev, O.; Kim, D.-W.; Gates, B. C. *J. Mol. Catal. A* **2000**, *162*, 67.

(53) Maloney, S. D.; Kelly, M. J.; Koningsberger, D. C. Gates, B. C. *J. Phys. Chem.* **1991**, *95*, 9406.

(54) Kawi, S.; Gates, B. C. *Inorg. Chem.* **1992**, *31*, 2939.

(55) Lai, F. S.; Gates, B. C. *Nano Lett.* **2001,** *1*, 583.

(56) Weber, W. A.; Phillips, B. L.; Gates, B. C. *Chem. Eur. J.* **1999**, *5*, 2899.

(57) Deutsch, S. E.; Miller, J. T.; Tomishige, K.; Iwasawa, Y. Weber, W. A.; Gates, B. C. *J. Phys. Chem.* **1996**, *100*, 13408.